Heavy-Higgs-boson production and W^-W^+ scattering processes in e^-e^+ collisions at high energy

John F. Gunion and A. Tofighi-Niaki
Department of Physics, University of California–Davis, California 95616
(Received 21 April 1987)

We employ exact matrix elements for the reactions $e^-e^+\to\nu\bar{\nu}W^-W^+$ and $e^-e^+\to e^-e^+W^-W^+$ to explore the observability of a standard-model Higgs boson and of W^-W^+ scattering processes at a high-energy e^-e^+ collider. We consider representative e^-e^+ center-of-mass energies of $\sqrt{s}=0.5$, 1, and 2 TeV.

I. INTRODUCTION

Observation of the Higgs boson of the standard $SU(2)_L\times U(1)$ model (SM) has been considered to be one of the primary goals for the next generation of e^-e^+ colliders.[1] Cross sections for Higgs-boson production and certain backgrounds have been considered in a variety of papers (see, for example, Refs. 1–3). For $m_H>2m_W$, however, the s-channel Higgs-boson diagram cannot be separated from the many other subprocesses contributing to the production of heavy-vector-boson pairs. Among these, vector-boson scattering reactions provide an important test of the SM in their own right. A study of Higgs-boson production in the WW channel at an e^-e^+ machine which included such diagrams in the effective-W approximation was carried out in Refs. 4 and 5. However, the accuracy of this approximation for the $m_H=\infty$ WW scattering continuum is uncertain,[6] and, in particular, is sensitive to the treatment of the Coulomb-pole contribution to WW scattering and whether or not transversely polarized initial W's are included. In addition, the full set of vector-boson scattering diagrams form only a small subset of all diagrams contributing to the production of vector-boson pairs. The additional subprocesses are of considerably less interest than Higgs-boson production and vector-boson scattering, but do require consideration. Indeed, when off-shell effects are allowed for, only the complete sum of contributing diagrams is gauge invariant and exhibits correct high-energy behavior.

Thus, in this paper we study the processes

$$e^-e^+\to\nu\bar{\nu}W^-W^+ \tag{1}$$

and

$$e^-e^+\to e^-e^+W^-W^+ , \tag{2}$$

employing exact gauge-invariant matrix elements. These are closely related to the ones obtained earlier for quark-initiated subprocesses.[7,8] The explicit forms we employ from Ref. 7 include the W^- and W^+ decays and all spin-density matrix correlations related thereto. We will use them to explore a variety of issues, such as (1) the exact level of the WW continuum, away from the Higgs resonance region, arising from reactions (1) and (2)—our results indicate a larger rate for continuum scattering than those of Ref. 4, (2) the most effective means for isolating the processes of greatest interest, namely, Higgs-boson production and WW scattering—in particular, means for reducing the two-photon collision "background," and (3) the best signal for longitudinally polarized W bosons.

II. GENERAL OVERVIEW

The general cross-section level for Higgs production via WW fusion is illustrated in Fig. 1 in the zero-width approximation of Ref. 2. Contributions from ZZ fusion are much smaller. We see that the cross section for a Higgs boson of given mass rises quickly beyond production threshold as $\sqrt{s}$ increases, rapidly reaching a level of the order of or larger than a tenth of a unit of R. At this cross-section level, one can imagine searching for the Higgs in the WW decay mode with both W's decaying hadronically, as well as in the mixed hadronic-leptonic decay modes for the two W's. Monte Carlo studies have found[9] that backgrounds to the pure hadronic final state from annihilation production of four-jets (with a total cross section of several units of R) can be greatly suppressed by two trivial means: requiring total energy deposited in the detector to be significantly less than $\sqrt{s}$; and requiring that the four jets cluster in two pairs, each having invariant mass near m_W. Similarly, the background from $e^-e^+\to W^-W^+$ is adequately suppressed by requiring that the W^-W^+ total mass be substantially less than $\sqrt{s}$. It is fortunate that the pure four-jet decay modes of the WW pairs from Higgs-boson production can be used since the mixed hadronic-leptonic final states have a considerably lower event rate. Considering only light-quark ($q=u,d,c,s$) channels and stable leptons ($l=e,\mu$), we find

$$2B(W^-\to q'\bar{q})B(W^+\to l^+\nu)\sim 0.16 . \tag{3}$$

However, in the hadronic modes it is not clear that we can determine the charge of a given W, and if the jet-jet mass resolution is not better than 10% we will have difficulty separating WW channels from ZZ channels. Thus, we will explore both the pure-hadronic and the mixed-mode channels.

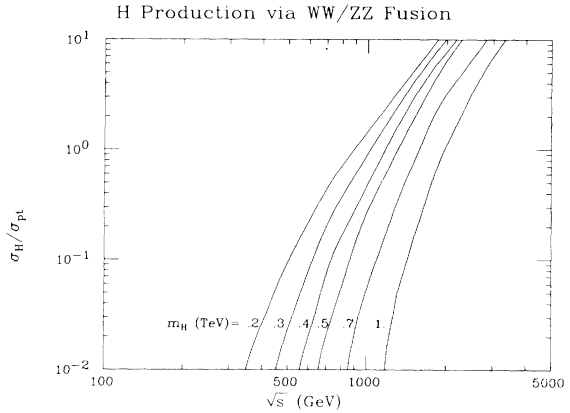

FIG. 1. We plot the Higgs cross section relative to $\sigma_{\rm pt}$ as a function of $\sqrt{s}$ for a variety of m_H values. The results are obtained using the techniques of Ref. 2.

In order to discuss the observability of a Higgs boson of a given mass, or of any other cross section, we shall assume that the machine design is such that in a year of operation the integrated luminosity is

$$L = 10^4 \times l/\sigma_{\rm pt} , \tag{4}$$

equivalent to

$$L = (1.15l \times 10^5 \text{ pb}^{-1}\text{yr}^{-1})[\sqrt{s} \text{ (TeV)}]^2 . \tag{5}$$

For a theorist's year of 10^7 sec this corresponds to an instantaneous luminosity of

$$\mathcal{L} = (1.15l \times 10^{34} \text{ cm}^{-2}\text{sec}^{-1})[\sqrt{s} \text{ (TeV)}]^2 . \tag{6}$$

If a given cross section is related to $\sigma_{\rm pt}$ by

$$\sigma = f\sigma_{\rm pt} , \tag{7}$$

and if the overall branching-ratio factor for seeing a particular final state of interest is B, then the number of events obtained in a year's running is

$$N_{\rm year} = 10^4 \times lfB . \tag{8}$$

From the plots of Fig. 1 we see that we obtain $>10^2 l$ Higgs-boson production events for $m_H = 300$ GeV at $\sqrt{s} \geq 430$ GeV, for $m_H = 500$ GeV at $\sqrt{s} \geq 625$ GeV, and for $m_H = 1$ TeV at $\sqrt{s} \geq 1.2$ TeV. Since cuts which eliminate backgrounds are certainly no more than 50% efficient for the Higgs signal, these are certainly the minimum energies at which one could hope to study production of a Higgs boson with the indicated masses.

We will use the exact matrix elements to examine in detail the three cases of (i) $m_H = 300$ GeV ($\Gamma_H = 9$ GeV) at $\sqrt{s} = 500$ GeV, (ii) $m_H = 500$ GeV ($\Gamma_H = 52$ GeV) at $\sqrt{s} = 1$ TeV, and (iii) $m_H = 1$ TeV ($\Gamma_H = 468$ GeV) at $\sqrt{s} = 2$ TeV.

In the first case we are near the production threshold and event rates for Higgs-boson production will be low, while in the third case, machine luminosity is unlikely to reach the $l = 1$ level but we are fairly far from threshold. We will find in all cases that discovery of the Higgs boson should be possible. Of course, since our exact matrix elements for process (1) contain not only the Higgs resonance but also WW scattering and other processes, we will simultaneously determine the level of the WW pair continuum, coming from these important sources, in the m_{WW} regions surrounding the Higgs peak. In fact, for the cases we have studied, this underlying WW continuum is closely approximated by that obtained by setting $m_H = \infty$. The perturbative tree-graph calculation of the WW scattering continuum at $m_H = \infty$ is also of great interest in its own right. First, at moderate values of $m_{WW} \lesssim 1$ TeV it provides an important testing ground for the standard-model gauge particle self-couplings. Second, if $m_H = \infty$, perturbatively computed WW scattering eventually violates unitarity in the region $m_{WW} \gtrsim 1$ TeV, and deviations because of nonperturbative effects should become evident as the WW scattering amplitudes become strong. Thus it is important to assess whether or not we can observe the WW scattering continuum. We find that crude measurements of this continuum for m_{WW} values in the vicinity of the above listed m_H values should be feasible at the indicated energies, except possibly in the first case.

In Fig. 2 we plot $d\sigma/dm_{WW}$ from reaction (1) for the three cases we shall consider. The only cuts imposed are that the four jets from the W decays have rapidities between -4 and $+4$. Also given is the level of the WW continuum in the case of an infinitely massive Higgs boson. The values we obtained here for the Higgs-boson production cross section at the peak, $m_{WW} = m_H$, are in very good agreement with those obtained in the effective-W approximation calculations of Ref. 4. However, we obtain quite different levels for the $m_H = \infty$ continuum. It is useful to tabulate the numbers of events available for further analysis. The excess of the Higgs peak over the WW continuum contains the following numbers of events in our three cases:

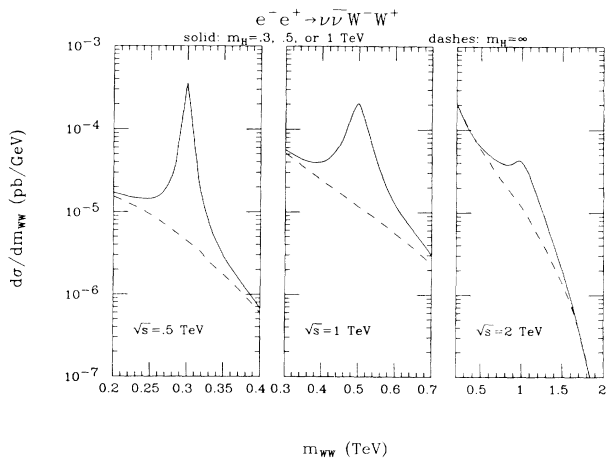

FIG. 2. We plot $d\sigma/dm_{WW}$ as a function of m_{WW} coming from reaction (1), for the three cases we consider. The only cuts imposed are that the four jets from the W decays have rapidities between -4 and $+4$. Also shown are results for $m_H = \infty$.

$$\text{No. of events in Higgs-boson peak} = \begin{cases} 150l\text{:}\ \ m_H = 0.3\ \text{TeV},\ \ \sqrt{s} = 0.5\ \text{TeV}, \\ 1900l\text{:}\ \ m_H = 0.5\ \text{TeV},\ \ \sqrt{s} = 1\ \text{TeV}, \\ 14000l\text{:}\ \ m_H = 1\ \text{TeV},\ \ \sqrt{s} = 2\ \text{TeV}. \end{cases} \tag{9}$$

Regarding the $m_H = \infty$ continuum level, let us compute the number of events obtained by integrating over m_{WW} from 0.2 to 0.4 TeV in case (i), from 0.3 to 0.7 TeV in case (ii), and from 0.5 to 1.5 TeV in case (iii). We obtain the following numbers of events:

$$\text{No. of } WW \text{ continuum events} = \begin{cases} 30l\text{:}\ \ 0.2 < m_{WW}(\text{TeV}) < 0.4,\ \ \sqrt{s} = 0.5\ \text{TeV}, \\ 760l\text{:}\ \ 0.3 < m_{WW}(\text{TeV}) < 0.7,\ \ \sqrt{s} = 1\ \text{TeV}, \\ 7400l\text{:}\ \ 0.5 < m_{WW}(\text{TeV}) < 1.5,\ \ \sqrt{s} = 2\ \text{TeV}. \end{cases} \tag{10}$$

Obviously the WW scattering continuum will be very difficult to measure in the first case, but might prove accessible in cases (ii) and (iii). It is also useful to compute the number of events in the WW scattering continuum within

$$\Delta m_{WW} = \max[0.05 m_H, \Gamma_H]\ , \tag{11}$$

around m_H as an estimate of this source of background underlying the Higgs-boson peak. We obtain

$$\text{No. of } WW \text{ continuum events} = \begin{cases} 7.5l\text{:}\ \ 0.292 < m_{WW}(\text{TeV}) < 0.308, \\ 65l\text{:}\ \ 0.448 < m_{WW}(\text{TeV}) < 0.552, \\ 1730l\text{:} 0.765 < m_{WW}(\text{TeV}) < 1.235. \end{cases} \tag{12}$$

These numbers should be compared to those given for the Higgs peak in Eq. (9) after multiplying the latter by a factor of 0.7, 0.5, or 0.5 for $m_H = 0.3$, 0.5, or 1 TeV, respectively, in order to correct for the restricted m_{WW} range.

Of course, m_{WW} can only be accurately determined in the case of the purely hadronic decay modes of the WW pair. For the mixed hadronic-leptonic decay mode there is an energetic missing neutrino. To determine m_{WW} we must first reconstruct its four-momentum. We have adopted the following procedure.

(1) Neglect the transverse momentum of the WW system and compute p_{T}^{ν} using the transverse momenta of the trigger lepton and the two jets from the hadronically decaying W.

(2) Assume that the lepton and missing neutrino momentum combine to yield a total four-momentum with square equal to $m_W{}^2$. Define

$$\alpha = m_W{}^2/2 - \mathbf{p}_T^l \cdot (\mathbf{p}_{\mathrm{T}}^1 + \mathbf{p}_{\mathrm{T}}^{j_1} + \mathbf{p}_{\mathrm{T}}^{j_2})$$

and

$$\delta = \alpha^2 - |\,\mathbf{p}_{\mathrm{T}}^l\,|^2\,|\,\mathbf{p}_{\mathrm{T}}^l + \mathbf{p}_{\mathrm{T}}^{j_1} + \mathbf{p}_{\mathrm{T}}^{j_2}\,|^2\ .$$

If $\delta > 0$ then we may solve for p_z^{ν} up to a twofold ambiguity. Choose that solution yielding the smallest value of m_{WW}. If $\delta < 0$ then we compute p_z^{ν} by taking $\delta = 0$. The reconstructed WW mass, m_{WW}^R, may then be calculated using p_z^{ν}. For later use we also define

$$\eta = \delta / m_W{}^4\ . \tag{13}$$

The resulting distribution in the reconstructed WW mass, denoted by m_{WW}^R, is shown in Fig. 3 in the case of $\sqrt{s} = 0.5$ TeV, for both $m_H = 0.3$ TeV and $m_H = \infty$, and in the case of $\sqrt{s} = 1$ TeV for $m_H = 0.5$ TeV and $m_H = \infty$. Obviously, the Higgs peak is considerably broadened, particularly in the first case. In addition, the m_{WW}^R distribution has a significant tail (summed in the last m_{WW}^R bin) extending beyond the nominal kinematic boundary. For the heavy Higgs boson of case (iii), $m_H = 1$ TeV, results are similar, but the broadening of the Higgs peak is smaller as a percentage of its nominal width.

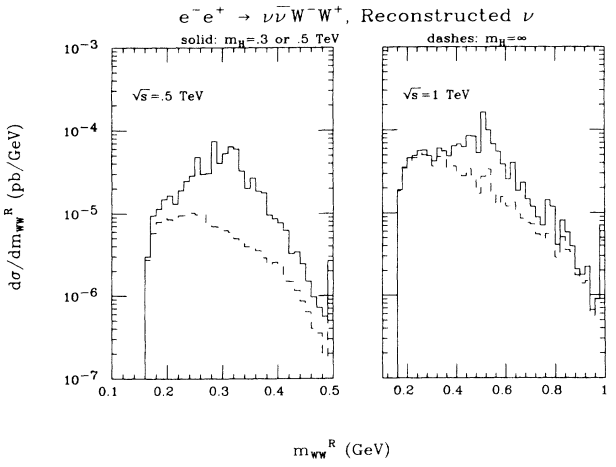

FIG. 3. We plot the reconstructed WW pair mass spectrum at $\sqrt{s} = 0.5$ TeV for $m_H = 0.3$ TeV and $m_H = \infty$, and at $\sqrt{s} = 1$ TeV for $m_H = 0.5$ TeV and $m_H = \infty$. The reconstruction of m_{WW} in the case of a missing neutrino is described in the text. The only cuts imposed are that the charged lepton from the one W and the two jets from the other W have rapidities between -4 and $+4$.

III. BACKGROUNDS AND CUTS

We have indicated earlier that at an e^-e^+ collider the backgrounds to the WW pair production reactions of interest, with m_{WW} significantly smaller than $\sqrt{s}$, must derive from processes in which a significant portion of the total $\sqrt{s}$ disappears. There are three obvious candidates, all of which have already been discussed in the literature:[2-5]

$$e^-e^+ \to \gamma W^-W^+ , \tag{14}$$

$$e^-e^+ \to \gamma\gamma W^-W^+ , \tag{15}$$

and

$$e^-e^+ \to e^-e^+\gamma\gamma : \gamma\gamma \to W^-W^+ . \tag{16}$$

The third process is, of course, one of the many types of reactions contained in the exact matrix elements for reaction (2). Monte Carlo studies again suggest[9] that processes in which a real W^-W^+ pair with $m_{WW} \ll \sqrt{s}$ is not produced, but rather is mimicked (e.g., by random four-jet production in 2γ collisions or $e^-e^+ \to \gamma + 4$ jets), are adequately suppressed by requiring that the four jets reconstruct to two pairs of jets, each pair having mass near m_W.

In order to gain an idea of the magnitude of the above real WW pair backgrounds we begin by presenting in Fig. 4 the cross sections for reactions (14) and (16), integrated over the m_{WW} range of $m_H - \Delta m_{WW}/2 < m_H + \Delta m_{WW}/2$ where Δm_{WW} is given in Eq. (11). [The cross section for reaction (15) was computed in Ref. 5, and is generally smaller than those we obtain for (14) and (16).] For this figure, the cross section for reaction (14) was obtained using the approximation given in Ref. 2, while that for (16) was computed in the simplest two-photon approximation (see Ref. 3). Without any cuts both backgrounds are large. Far from threshold, i.e., m_{WW} significantly smaller than $\sqrt{s}$, background (16) is largest, but in the region of $\sqrt{s}$ and m_{WW} of interest to us these backgrounds are comparable. However, it has been emphasized in Refs. 2, 3, and 5 that the W's from all these reactions tend to be produced at small angles with respect to the beam direction. Let us define θ^*_{eW} to be the angle between the incoming e^- and the outgoing W^-, *in the WW center of mass.* Then, in the approximate calculations referred to above, a simple cut of the form $|\cos\theta^*_{eW}| < z_0$ with, for example, $z_0 = 0.7$ reduces these backgrounds substantially (see Fig. 4). The Higgs signal is essentially flat in $\cos\theta^*_{eW}$ and is reduced relatively little in comparison. However, this type of cut has several disadvantages.

(a) The W's produced via WW scattering processes also tend to be produced along the beam directions, and are severely suppressed by this same cut. Measurement of the $m_H = \infty$ continuum would not be possible.

(b) The mixed hadronic-leptonic WW decay channel requires reconstruction of the WW center of mass in order to define θ^*_{eW}, a process which smears out the distribution in $\cos\theta^*_{eW}$.

(c) Some of the background subprocesses other than $\gamma\gamma \to W^-W^+$ contained in reaction (2) are not as efficiently removed by this cut.

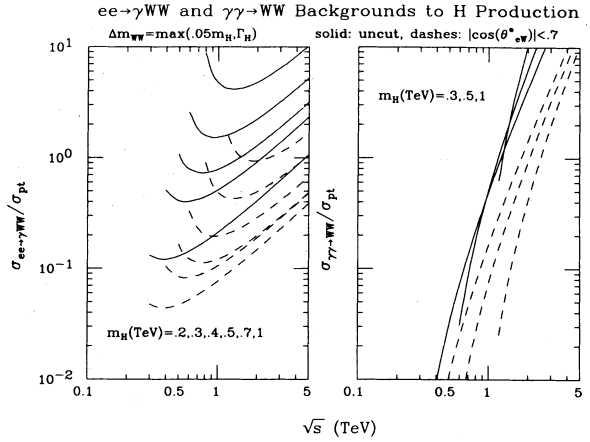

FIG. 4. The cross sections for reactions (14) and (16) (denoted by $\sigma_{\gamma\gamma\to WW}$) integrated over the m_{WW} range of $m_H - \Delta m_{WW}/2 < m_H + \Delta m_{WW}/2$ where Δm_{WW} is given in Eq. (11). [The cross section for reaction (15) tends to lie below these two.] The results without any cuts and with a cut on the angle of the outgoing W^- with respect to the incoming e^- (defined in the WW center of mass), $|\cos\theta^*_{eW}| < 0.7$, are given for the indicated values of m_H. In the uncut case these should be compared with the cross sections of Fig. 1 times 0.7, 0.5, 0.5 for $m_H = 0.3$, 0.5, 1 TeV, respectively (to correct for the m_{WW} restriction). In the presence of the $|\cos\theta^*_{eW}| < 0.7$ cut the cross sections of Fig. 1 should be reduced by a further factor of 0.7 before comparison.

A much more ideal procedure would be to trigger on the $\nu\bar{\nu}$ spectators of the reaction (1) of interest. Since this is impossible, we adopt the converse approach of antitriggering on the e^-, e^+, and γ spectators of reactions (14), (15), and (16). Our approach assumes that the m_{WW} range of interest is significantly below $\sqrt{s}$ so that these spectators will tend to be energetic. Only those background events where all spectators either have low momentum or disappear in the extreme forward or backward detector holes cannot be directly eliminated. In the following we develop a strategy for severely limiting even these background events. It tends to be more effective than the $\cos\theta^*_{eW}$ cuts in isolating the Higgs signal, while avoiding the associated problems. We have investigated this strategy in detail for the full set of background reactions contained in (2). Our exact matrix elements for reaction (2) include the most serious of the three backgrounds discussed above: namely, the two-photon collision background (16). Closely analogous procedures and results can be anticipated for the background processes (14) and (15). The strategy hinges upon having good detector coverage such that either (or both) the final e^- or e^+ of process (2), and similarly the γ's of processes (14) and (15), would be detectable if emerging with laboratory angle and transverse momentum greater than specific minimum values. In our study of reaction (2) we have assumed that an e^- or e^+ with laboratory angle larger than 20 degrees *and* transverse momentum larger than 25 GeV would be detectable; i.e., events from reaction (2) are accepted, in all that follows,

as true background events only if

$$\theta_s^{\text{lab}} < 20^\circ \text{ or } p_T^s < 25 \text{ GeV} , \tag{17}$$

for both the outing $s = e^-$ and $s = e^+$ spectators. We regard these values as being on the pessimistic side.

The idea is then very simple. The processes of interest, both Higgs-boson production and WW scattering, tend to produce WW pairs with very substantial transverse momentum, while the backgrounds as well as the many uninteresting subprocesses contributing to (1), will be characterized by rather limited transverse momentum. For the pure hadronic decay mode of the W's this transverse momentum can be directly measured. For the mixed hadronic-leptonic WW decay channels we cannot directly measure the WW pair transverse momentum; however, we are much more likely to find an allowed solution for p_z^ν [i.e., $\eta > 0$, see Eq. (13), is much more likely] for the background processes with limited WW transverse momentum than for the reaction (1). Before proceeding we note that a fully reliable investigation of the type of transverse motion cuts which we propose can only be carried out using complete matrix elements for the reaction (1) and (2).

The reader should be warned that the results we present for reaction (2) are based on (roughly) only ten thousand events accepted subject to the cuts (17); and typically only two thousand events remain after the p_T^{WW} or η cuts given below. Thus exact cross sections and distributions given for this background will not be perfectly accurate. However, the general magnitudes and shapes seem to be reliable. The statistical accuracy of the results for process (1) is far higher, with an order of one-hundred thousand events contributing after the cuts discussed below.

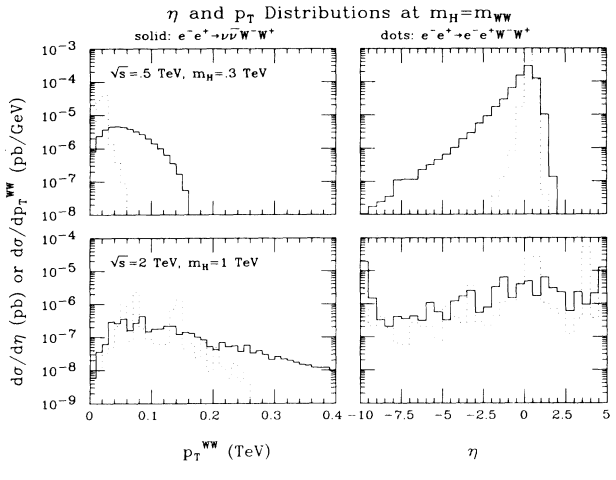

FIG. 5. Distributions in p_T^{WW} and η at $m_{WW} = m_H$, for cases (i) and (iii), coming from reactions (1) and (2) [the latter being subjected to the requirements of Eq. (17)]. The $m_H = \infty$ distributions are quite similar. Distributions for case (ii) resemble those for case (i) except that they are somewhat broader in both variables.

We begin by plotting in Fig. 5 the distributions in p_T^{WW} and η [see Eq. (13)], at $m_{WW} = m_H$, resulting from reactions (1) and (2). Explicit results are presented for cases (i) and (iii) with the Higgs resonance present. Distributions for case (ii) are very similar to those for case (i), after rescaling to account for the higher Higgs-boson mass and $\sqrt{s}$. Distributions for $m_H = \infty$ are, for all three cases, very similar to those found when sitting on the Higgs resonance peak. In case (i) the efficacy of a cut in either p_T^{WW} or η is evident, with optimum values easily read off the graphs. In case (iii) the distributions are not as sharply distinct, but, again, it is obvious that the process (1) has a very long tail at high p_T^{WW} and at negative values of η whereas the background process (2) has restricted p_T^{WW} and has most of its weight in the positive η region. Based on these distributions, and similar ones for case (ii), we find that good choices for cut boundaries are (i) $p_T^{WW\,\min} = 50$, 90, and 150 GeV, and (ii) $\eta^{\max} = -0.25$, -1.5, and -2.0, for the choices of Higgs-boson mass and $\sqrt{s}$ values of cases (i), (ii), and (iii), respectively. Since p_T^{WW} and η cuts are very closely related we shall only consider imposing one or the other. Other variables which we may wish to consider restricting are $\cos\theta_{eW}$, the *laboratory* angle between the incoming e^- and outgoing W^-, and $y^-(y^+)$ the laboratory rapidity of the outgoing $W^-(W^+)$. The processes of interest from reaction (1) tend to yield events with small y^- and y^+, and with a flat $\cos\theta_{eW}$ distribution, whereas background processes give broad y^- and y^+ distributions and peak near $\cos\theta_{eW} = \pm 1$. However, cuts in these latter variables alone are completely inadequate for eliminating the background from reaction (2) and they will only be considered in combination with cuts on p_T^{WW} or η.

In fact, it is convenient to create a list of possible cuts: (1) $p_T^{WW} > p_T^{WW\,\min}$, (2) $p_T^{WW} > p_T^{WW\,\min}$ and $|\cos\theta_{eW}| < 0.7$, (3) $p_T^{WW} > p_T^{WW\,\min}$ and $|y^-|, |y^+| < 1.5$, (4) $\eta < \eta^{\max}$, (5) $\eta < \eta^{\max}$ and $|y^-|, |y^+| < 1.5$. In all cases we require that the observable jets or lepton from the W decays have laboratory rapidities between -4 and $+4$.

In Fig. 6 we give the value of $d\sigma/dm_{WW}$ at $m_{WW} = m_H$ for reactions (1) and (2) after imposing the various cuts listed above, in cases (i), (ii), and (iii). From these results the efficiency and effectiveness of each of the cuts may be judged. Our goal is to achieve a relatively efficient cut [i.e., one that does not remove too much of the reaction (1) signal] which effectively eliminates the reaction (2) background. In terms of the symbols of the plots we require either that the square be substantially below the diamond (for a Higgs resonance being present) or that the plus be below, or at least no larger than, the cross (for $m_H = \infty$). A glance at the plots indicates immediately the effectiveness of the p_T^{WW} and η cuts, given that the background starts at a level which is much above the upper limits of the graphs. We also note that the combination cuts No. 2 and No. 5 begin to reveal a small (but obviously unusable) Higgs-boson signal in the background process (2). We will analyze each of our three cases in detail. An overall summary of the results

outlined below appears in Tables I and II. Before proceeding we note that in discussing the mixed decay modes we will neglect m_{WW} reconstruction. The reader should keep in mind that for these modes the net number of events obtained in the specified m_{WW} bins would actually be spread out over a somewhat larger range in the reconstructed WW mass, m_{WW}^R.

In case (i) we see that the p_T^{WW} or η cuts, No. 1 or No. 4, achieve background rejection with good efficiency. Since we had only $\sim 150l$ Higgs events and $\sim 30l$ WW continuum events (for 0.2 TeV $< m_{WW} <$ 0.4 TeV) to begin with this is fortunate. Let us imagine that all purely hadronic WW decay modes (net $B = \frac{9}{16}$) and mixed hadronic-leptonic modes with light quarks and a stable charged lepton (net $B = 0.16$) are usable, and employ the p_T^{WW} cut in the first instance and the η cut in the second. From Fig. 6 we find that if a Higgs boson is present the efficiency weighted B is ~ 0.32 in the pure hadronic mode and ~ 0.05 for the mixed mode. The mixed channel is clearly very marginal but the pure hadronic mode channel should provide a reasonable signal. In both cases background at the Higgs peak will be very small. The $m_H = \infty$ WW scattering continuum has efficiency weighted branching ratios of ~ 0.39 and ~ 0.05 in the pure hadronic and mixed decay channels, respectively, resulting in rather few background free events-boson.

Turning to case (ii) we recall that we begin with $1900l$ Higgs-boson events and $760l$, $m_H = \infty$ WW scattering continuum events. Again a pure p_T^{WW} or η cut suffices to reveal the Higgs resonant peak or, in its absence, the WW scattering continuum. For $m_{WW} = m_H = 0.5$ TeV, the pure hadronic channel has an efficiency weighted B of ~ 0.23, and the mixed mode channel, ~ 0.05. Thus even the mixed modes contain some $95l$ events in the Higgs peak after cuts, above a very much smaller background. The efficiency-weighted B's for the $m_H = \infty$ continuum are even larger; ~ 0.32 for the pure hadronic modes with cut No. 1, and ~ 0.065 for the mixed mode with cut No. 4. Clearly we are left with a significant number of usable WW scattering continuum events in the WW pair mass region 0.3 TeV $\leq m_{WW} \leq$ 0.7 TeV. For instance, in the pure hadronic WW decay mode we have $\sim 240l$ WW scattering events compared to a background from reaction (2) of $\sim 95l$. One could even imagine imposing a combination cut, such as No. 2, yielding $\sim 95l$ hadronic mode WW scattering continuum events over a background of $\sim 30l$. However, even if $l = 1$ is achievable, no improvement of the signal's statistical significance results despite the improved ratio of signal over background.

In our final sample case (iii), the efficiencies of our p_T^{WW} and η cuts are smaller, as one might anticipate from Fig. 5. However, even if the integrated luminosity is characterized by only $l = 0.25$, the surviving number of events is competitive with the previous case. At $l = 0.25$ we begin with 3500 Higgs peak events, and 1850 WW scattering events in the range 0.5 TeV $\leq m_{WW} \leq$ 1.5 TeV. At the Higgs peak we obtain efficiency weighted B's for process (1) of ~ 0.17 for the pure hadronic mode and cut No. 1 and of ~ 0.06 for the mixed mode and cut

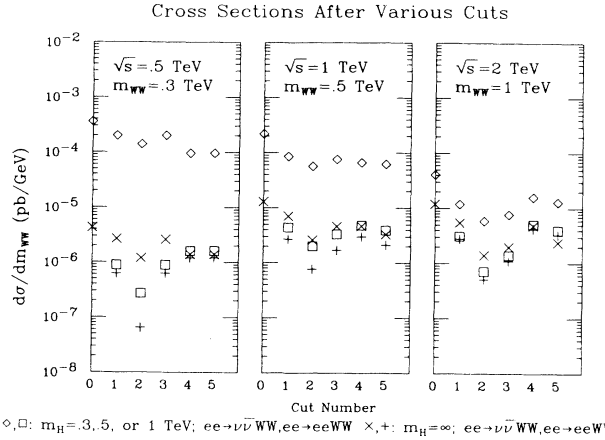

FIG. 6. In this figure we give the cross section $d\sigma/dm_{WW}$ at $m_{WW} = 0.3$ TeV and $\sqrt{s} = 0.5$ TeV, at $m_{WW} = 0.5$ TeV and $\sqrt{s} = 1$ TeV, and at $m_{WW} = 1$ TeV and $\sqrt{s} = 2$ TeV, for reactions (1) and (2) after imposing various cuts as listed in the text. Results are given both in the presence of a Higgs boson with $m_H = m_{WW}$ [indicated by the diamonds and squares for reactions (1) and (2), respectively] and for $m_H = \infty$ [indicated by the crosses and pluses for reactions (1) and (2), respectively]. Also given in each case, as the cut number=0 values, are the uncut cross sections for reaction (1) both for $m_H = m_{WW}$ (diamond) and for $m_H = \infty$ (cross).

No. 4. For $l = 0.25$ these correspond to ~ 600 pure hadronic mode and ~ 210 mixed mode events in the Higgs peak, with small backgrounds. At $m_H = \infty$ the corresponding efficiency weighted B's are ~ 0.25 for the hadronic mode and ~ 0.07 for the mixed mode. For $l = 0.25$, the m_{WW} bin specified above contains ~ 460 hadronic mode events and ~ 130 mixed mode events, with backgrounds of ~ 230 and ~ 115, respectively.

We present a survey of the resulting efficiency and branching ratio weighted event rates in Tables I and II. In Table I we give the rates for $ee \to \nu\bar{\nu}H(\to WW)$ (integrated over the entire Higgs peak) and for $ee \to \nu\bar{\nu}WW$ and $ee \to eeWW$ at $m_H = \infty$ integrated over the m_{WW} ranges specified in Eq. (10). Results are presented for all three energies and for both the pure hadronic mode with cut No. 1 imposed and the mixed mode with cut No. 4 imposed. This Table indicates that measurement of the $m_H = \infty$ WW scattering continuum of reaction (1) over the background reaction (2) will be feasible for the higher two $\sqrt{s}$ values we consider, provided backgrounds we have not considered, e.g., from random hadronic jet production, can be equally suppressed.

In Table II we present results for the efficiency and branching ratio weighted hadronic mode events for the above three cases, but with m_{WW} restricted to lie within $\pm\Delta m_{WW}/2$ [see Eq. (11)] of the m_H value we have chosen to explore at each given energy. This Table is appropriate for assessing backgrounds to Higgs-boson detection in the pure hadronic mode coming from the underlying $m_H = \infty$ WW continuums of reactions (1) and (2). Table II makes it clear that Higgs-boson detection will be relatively straightforward unless other back-

TABLE I. We tabulate event rates for the pure hadronic WW decay modes (with the indicated $p_T^{WW\,\min}$ cut in units of GeV) and for the mixed hadronic-leptonic decay modes (with the indicated $\eta^{\max}$ cut). The event rates incorporate efficiency weighted branching ratios and are obtained by integrating over the indicated m_{WW} ranges. The "H peak" event rate is the number of events in the presence of a given Higgs resonance peak that is in *excess* of the number of events obtained for $m_H=\infty$. The multiplier l specifies the luminosity according to the definition of Eqs. (5) and (6).

	$ee\to\nu\bar{\nu}WW$ H peak: $m_H=0.3$ TeV	$ee\to\nu\bar{\nu}WW$ $m_H=\infty$	$ee\to eeWW$ $m_H=\infty$
	$\sqrt{s}=0.5$ TeV, $(0.2<m_{WW}\ (\text{TeV})<0.4)$		
Hadronic ($p_T^{\min}=50$)	$48l$	$12l$	$3l$
Mixed ($\eta^{\max}=-0.25$)	$9l$	$1.5l$	$1.4l$
	$\sqrt{s}=1$ TeV, $(0.3<m_{WW}\ (\text{TeV})<0.7)$		
	$ee\to\nu\bar{\nu}WW$ H peak: $m_H=0.5$ TeV	$ee\to\nu\bar{\nu}WW$ $m_H=\infty$	$ee\to eeWW$ $m_H=\infty$
Hadronic ($p_T^{\min}=90$)	$440l$	$240l$	$95l$
Mixed ($\eta^{\max}=-1.5$)	$95l$	$50l$	$35l$
	$\sqrt{s}=2$ TeV, $(0.5<m_{WW}(\text{TeV})<1.5)$		
	$ee\to\nu\bar{\nu}WW$ H peak: $m_H=1$ TeV	$ee\to\nu\bar{\nu}WW$ $m_H=\infty$	$ee\to eeWW$ $m_H=\infty$
Hadronic ($p_T^{\min}=150$)	$2380l$	$1850l$	$940l$
Mixed ($\eta^{\max}=-2.0$)	$840l$	$520l$	$460l$

TABLE II. We tabulate the number of events in the purely hadronic decay modes of the WW pair, after imposing the indicated $p_T^{WW\,\min}$ cut on the WW transverse momentum. The event numbers incorporate the appropriate efficiency weighted branching ratio and correspond to integrating over the indicated m_{WW} range. The "H peak" event rate is the number of events in the presence of a given Higgs resonance peak that is in *excess* of the number of events obtained for $m_H=\infty$. The multiplier l specifies the luminosity according to the definition of Eqs. (5) and (6). The m_{WW} range is chosen so that a comparison of the H peak rate with the sum of the two $m_H=\infty$ rates gives a rough indication of the significance of the Higgs signal with respect to the WW continuum backgrounds from reactions (1) and (2).

	$m_H-\Delta m_{WW}/2<m_{WW}<m_H+\Delta m_{WW}/2$ H peak $m_H=0.3$, 0.5, or 1	$ee\to\nu\bar{\nu}WW$ $m_H=\infty$	$ee\to eeWW$ $m_H=\infty$
$\sqrt{s}=0.5$ TeV ($p_T^{\min}=50$)	$34l$	$3l$	$1l$
$\sqrt{s}=1$ TeV ($p_T^{\min}=90$)	$220l$	$20l$	$8l$
$\sqrt{s}=2$ TeV ($p_T^{\min}=150$)	$1190l$	$430l$	$220l$

grounds, such as random four-jet production processes are more important than those given.

To summarize, we see that the p_T^{WW} and η cuts No. 1 and No. 4, are of primary utility. Cuts in $\cos\theta_{eW}$ and y alone do not yield adequate signal to background ratios. Combination cuts involving p_T^{WW} or η and $\cos\theta_{eW}$ or $y^{\pm}$, generally merely reduce the event rate without significantly improving the statistical significance of the signal. Indeed, our results indicate that a detector with limited $\cos\theta_{eW}$ or $y^{\pm}$ acceptance would be undesirable, both from this standpoint and that of not allowing imposition of our basic background cuts (17).

Finally, since the resulting purely hadronic mode event rates are relatively modest, it is important to return to the question of whether this mode can, in fact, be used in the presence of random four-jet backgrounds from $\gamma\gamma$ scattering, $e^-e^+\to\gamma\gamma+4$ jets and e^-e^+ annihilation events with substantial energy in the beam pipes and/or detector holes. Aside from the earlier mentioned reduction in these backgrounds obtained by looking for two pairs of jets, each with pair mass near m_W, it is important to recognize that the p_T^{WW} and η cuts are probably nearly as effective in eliminating these backgrounds as they are in eliminating the true WW backgrounds. A detailed Monte Carlo study is clearly desirable, and is in progress,[9] but beyond the scope of the present work. It should also be noted that both the signal rate would worsen and the random four-jet backgrounds would increase if there is substantial probability that the colliding e^- and e^+ will have lost energy as part of the bunch crossing process. It is probable that if the total energy loss averages more than 25% observation of Higgs-boson production would be severely impacted and detection of WW scattering would become impossible.

IV. SIGNALS FOR LONGITUDINAL W's

In the preceding considerations we have not made any use of one of the primary signals for a WW pair from the decay of a Higgs boson—namely, the longitudinal polarization of both W's. In this section we wish to explore several ways for recognizing longitudinally polarized W's, and, in the process, demonstrate that still further, highly efficient cuts against the continuum component of the backgrounds, all of which primarily produce transversely polarized W's, are possible. Of course, these cuts will not be useful in isolating the WW scattering continuum in the $m_H=\infty$ case, since it also contains primarily transversely polarized W's in the energy and m_{WW} range being considered.

One technique for recognizing a longitudinally polarized W boson has been particularly stressed in Ref. 10. If we define the angle θ^* to be the angle *in the W rest frame* of one W decay product with respect to the direction of motion of the W in the laboratory, a longitudinally polarized W will have a decay distribution of the form

$$\sin^2\theta^* , \tag{18}$$

while averaging over the two helicities corresponding to transverse W polarization yields

$$1+\cos^2\theta^* . \tag{19}$$

That (18) really is typical of Higgs-boson decay, while (19) is dominant for both WW scattering continuum processes and the $m_H=\infty$ component of the background reaction (2) is illustrated in Fig. 7. There we focus on case (ii) and present plots of $d\sigma/d\,|\cos\theta^*|$, after the imposition of the p_T^{WW} cut No. 1.

A different, and apparently more powerful discrimination between longitudinally and transversely polarized W's produced by processes of the type being considered was developed in Ref. 11. We first define the variables

$$r_T^{\max}\equiv\frac{p_T^{\max}}{m_{WW}},\quad r_T^{\min}\equiv\frac{p_T^{\min}}{m_{WW}} , \tag{20}$$

where $p_T^{\max}(p_T^{\min})$ is the transverse momentum of the W decay jet with largest (smallest) transverse momentum with respect to the collision axis. For the purely hadronic decay mode we first boost to the WW center of mass before computing $r_T^{\min}$ and $r_T^{\max}$. For the mixed decay mode we define $r_T^{\min}$ and $r_T^{\max}$ in the laboratory frame. We will give results for the former case, in the presence of the p_T^{WW} cut No. 1. (Results for the latter case, with the η cut No. 4 imposed, are not very different.) Before proceeding, let us recall that longitudinally polarized W's tend to decay to two jets with momenta of similar magnitude in the moving W frame. In contrast, transversely polarized W's prefer to decay in such a way that one jet is emitted opposite the W direction of motion, while the other is along the direction of motion, resulting in one hard and one soft jet. As a result, a sharp distinction between energetic W's polarized longitudinally and ones polarized transversely emerges through correlations in the two-dimensional $r_T^{\max}-r_T^{\min}$ space. Decays of a longitudinally polarized W populate a region along a line of constant $r_T^{\max}+r_T^{\min}$, with few events at small $r_T^{\min}$. In contrast, decays of a transversely polarized W accumulate near $r_T^{\min}=0$ over a range of

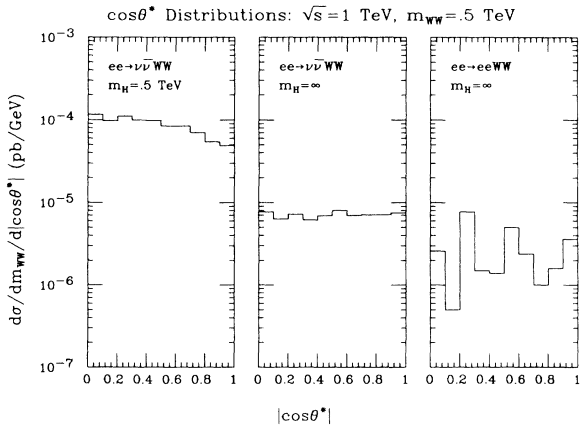

FIG. 7. Plots at $m_{WW}=0.5$ TeV and $\sqrt{s}=1$ TeV of $d\sigma/d\,|\cos\theta^*|$, after the imposition of the p_T^{WW} cut No. 1. The distributions from reaction (1) for $m_H=0.5$ TeV and for $m_H=\infty$ are presented, as well as that from reaction (2) for $m_H=\infty$.

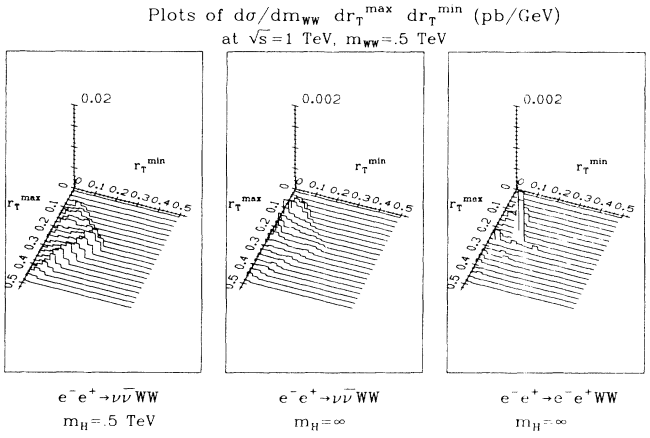

FIG. 8. We present three-dimensional plots in $r_T^{\min}$-$r_T^{\max}$ space for the same three situations considered in Fig. 7.

$r_T^{\max}$. This is illustrated in Fig. 8 where we present three-dimensional plots in $r_T^{\min}-r_T^{\max}$ space for the same three situations considered in Fig. 7. In order to further illustrate the differences between the Higgs-boson signal and the WW scattering continuum and $ee\to eeWW$ backgrounds it is useful to take a slice through the three-dimensional plots at fixed $r_T^{\max}$. Plots for such a slice are given in Fig. 9. The peaking of the Higgs-resonance events at large values of $r_T^{\min}$ is apparent. These plots demonstrate that by retaining only events with

$$r_T^{\max}+r_T^{\min}>r_{\rm sum},\quad r_T^{\min}>r_{\min}\ , \tag{21}$$

one can further enhance the Higgs-boson decays relative to background events with good efficiency. We have not attempted to optimize such a cut but $r_{\rm sum}=0.35$ and $r_{\min}=0.125$ would be typical choices.

For an infinitely massive Higgs boson and at values of m_{WW} in the TeV range, accessible for $\sqrt{s}\gtrsim 2$ TeV, one

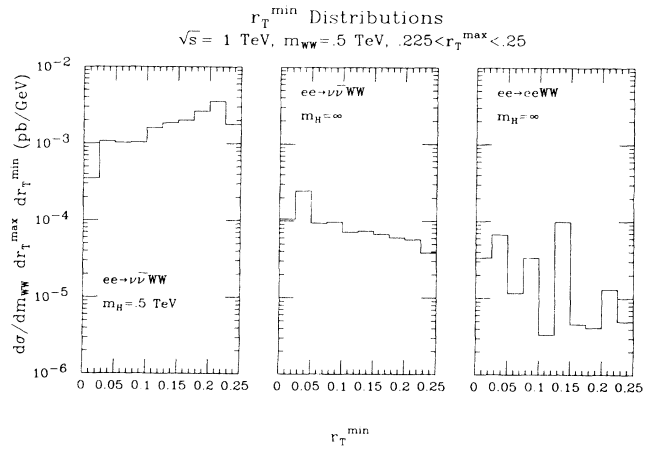

FIG. 9. We plot $d\sigma/dm_{WW}dr_T^{\max}dr_T^{\min}$ (in pb/GeV) at fixed $m_{WW}=0.5$ TeV, for the $r_T^{\max}$ bin specified by $0.225\le r_T^{\max}\le 0.25$, as a function of $r_T^{\min}$. The three graphs represent fixed-$r_T^{\max}$ slices of the three-dimensional plots of Fig. 8.

might hope that the $W_LW_L\to W_LW_L$ portion of the WW scattering amplitudes would begin to emerge over the contributions involving one or more transversely polarized W's. However, for the $m_H=\infty$, $\sqrt{s}=2$ TeV case which we have studied, the $\cos\theta^*$ and $r_T^{\min}-r_T^{\max}$ distributions are very similar to those we have presented for the $m_H=\infty$, $\sqrt{s}=1$ TeV case. They do not give any visible indication of longitudinal polarization for the final W's. Further investigation is required to determine how high in energy and WW mass it will be necessary to go before longitudinal modes will become observable.

Finally we note that in the Superconducting Super Collider studies of Ref. 11 it was found that random jet backgrounds tended to be even more peaked at small $r_T^{\min}$ than transversely polarized W's. Anticipating that the same will be true here it is clear that the cuts of Eq. (21) are likely to provide another powerful means for eliminating such backgrounds to WW pairs coming from Higgs-boson decay.

V. BEAM POLARIZATION

It is conceivable that beam polarization could be of considerable utitility in separating the Higgs boson or WW scattering continuum from random jet backgrounds. Higgs-boson production, WW scattering and, indeed, all processes contributing to reaction (1) derive, of course, entirely from the left-handed e^-'s and right-handed e^+'s in the colliding beams. They can be turned on and off by an appropriate helicity choice for either beam. In contrast, backgrounds deriving from random jet production, as opposed to real W production, are likely to be insensitive to beam polarization. However, backgrounds deriving from real W's may behave in a similar fashion to the processes of interest. For instance, many of the uninteresting diagrams contributing to reaction (2) involve W bremsstrahlung from the beam particles. These could be just as important as the polarization insensitive two-photon diagrams once the p_T^{WW} or η cut is imposed, and will, of course, be turned on and off in the same manner as the subprocesses of interest. Measurement of the m_{WW} spectrum using, for example, a right-handed e^- beam would then not yield a reliable background determination if this type of real WW background is important.

We have pursued this question by exploring the sensitivity of reaction (2) to beam polarization. We have recomputed the cross section $d\sigma/dm_{WW}$ at $m_{WW}=0.5$ TeV and $\sqrt{s}=1$ TeV from reaction (2) (after cuts) for a purely right-handed polarized e^- beam, and compared to our unpolarized beam results. We define the $ee\to eeWW$ cross-section ratio

$$R_{\rm pol}\equiv\frac{\dfrac{d\sigma^{e_R^-}}{dm_{WW}}}{\dfrac{1}{2}\left[\dfrac{d\sigma^{e_R^-}}{dm_{WW}}+\dfrac{d\sigma^{e_L^-}}{dm_{WW}}\right]}\ , \tag{22}$$

and evaluate R_{pol} after imposing the three cuts involving p_T^{WW}—No. 1, No. 2, and No. 3—and find

$$R_{\rm pol}=\begin{cases}0.56\ (0.3),\ \text{cut No. 1},\\ 0.65\ (0.36),\ \text{cut No. 2},\\ 0.63\ (0.34),\ \text{cut No. 3},\end{cases} \tag{23}$$

where the first number is the value for $m_H=0.5$ TeV and the second number (in parentheses) is for $m_H=\infty$. Obviously the background from reaction (2) remaining after our cuts is rather sensitive to beam polarization and will decrease substantially for a purely right-handed e^- beam polarization. Thus determination of the reaction (2) background to Higgs-boson production and the WW scattering continuum using beam polarization will require relying on theoretical computations, such as the present one, of its sensitivity to beam polarization. We anticipate that a similar statement applies to other backgrounds which produce real W's.

VI. CONCLUSIONS

We conclude that observation of a standard-model Higgs boson produced via $e^-e^+\to\nu\bar{\nu}H$ with $m_H>2m_W$ will be relatively straightforward at an e^-e^+ collider with energy $\sqrt{s}$ roughly a factor of 2 above m_H. Efficient techniques for eliminating the background from two-photon scattering and other processes contained in $e^-e^+\to e^-e^+W^-W^+$, based on antitriggering on spectators and requiring large transverse momentum for the WW system, have been given. These techniques require that we are focusing on a region of m_{WW} substantially below $\sqrt{s}$. They make feasible the use of both the purely hadronic and the mixed hadronic-leptonic WW decay modes. Decay product correlations for longitudinally polarized W's from Higgs-boson decay have been detailed, and will provide a clear signature that the cuts have indeed isolated the Higgs boson.

The same background elimination procedures may also make measurement of the WW scattering continuum possible, at least for $\sqrt{s}\gtrsim 1$ TeV. However, in the cases we have studied, this continuum is dominated by transversely polarized W's and W decay product distributions will not provide a final proof that we have isolated this class of events.

In both cases, backgrounds from processes which produce random four jets, such as $\gamma\gamma\to 4$ jets, $e^-e^+\to\gamma\gamma+4$ jets, or $e^-e^+\to 4$ jets (with missing energy in the detector holes) are likely to be greatly reduced by employing the same techniques which eliminate the uninteresting direct WW production backgrounds in combination with the requirement that the four jets come in two pairs with mass in the vicinity of m_W (Ref. 9). The exact level of reduction possible here will determine whether or not the WW scattering continuum will be measureable.

The role that beam polarization can play in separating Higgs-boson production and WW scattering from backgrounds is uncertain. It is clear that these processes of interest will be turned off for a purely right-handed polarization of the incoming e^- beam, while random jet backgrounds are probably little affected. But the latter does not seem to be true of backgrounds producing real WW pairs. We have found that once cuts have been imposed to eliminate the bulk of the primary real WW pair background, $ee\to eeWW$, the remaining part is rather sensitive to beam polarization and, in particular, decreases substantially for a purely right-handed e^- beam. Undoubtedly, this is largely because of the fact that cuts designed to eliminate the two-photon process inevitably enhance the relative importance of the more polarization sensitive type of diagrams contained in the full sum of *all* matrix element contributions to reaction (2). We thus conclude that beam polarization is likely to be of greatest utility if random jet backgrounds are dominant.

We end by reiterating that for the observation of either the Higgs boson or the WW scattering processes it is important that there not be too much degradation of the initial collision energy as a result of the bunch crossing dynamics. This is especially crucial for observation of the WW scattering continuum, which is relatively easily obscured by such effects, but is also important for detection of a Higgs resonance. Maximum effort on the part of machine designers to avoid beam energy loss is appropriate.

ACKNOWLEDGMENTS

We would like to thank the Department of Energy for support. This work was performed as part of the e^-e^+ linear collider study sponsored by the Standord Linear Accelerator Center. We are indebted to all the members of that study group for helpful comments, in particular, D. Burke, G. Feldman, and A. Peterson.

[1]See, for example, the LEP 200 study by J. Boucrot *et al.*, Report No. CERN-EP/87-40, 1987 (unpublished) and the pioneering article by D. R. T. Jones and S. T. Petcov Phys. Lett. **84B**, 440 (1979).

[2]S. Dawson and J. Rosner, Phys. Lett. **148B**, 497 (1984). In our applications of their formulas we have corrected several typographical errors for $e^-e^+\to W^-W^+$.

[3]K. Hikasa, Phys. Lett. **164B**, 385 (1985). The result quoted in this paper for the integrated $\gamma\gamma\to W^-W^+$ cross section has an incorrect sign for one term.

[4]G. L. Kane and J. J. G. Scanio Nucl. Phys. **B291**, 221 (1987).

[5]M. C. Bento and C. H. Llewellyn Smith, Nucl. Phys. **B289**, 36 (1987).

[6]J. F. Gunion, J. Kalinowski, A. Tofighi-Niaki, A. Abbasabadi, and W. Repko, in Proceedings of the Summer Study on the Design and Utilization of the Superconducting Super Collider, Snowmass, Colorado, 1986, edited by R. Donaldson and Jay Marx (Division of Particles and Fields, American Physical Society, New York, to be published).

[7]J. F. Gunion, J. Kalinowski, and A. Tofighi-Niaki, Phys. Rev.

Lett. **57**, 2351 (1986).
[8]D. Dicus and R. Vegas, Phys. Rev. Lett. **57**, 1110 (1986).
[9]These are being performed by members of the e^-e^+ Study Group at Stanford Linear Accelerator Center—in particular, by D. Burke and A. Peterson.
[10]M. Duncan, G. Kane, and W. Repko, Nucl. Phys. **B272**, 517 (1986).
[11]J. F. Gunion and M. Soldate, Phys. Rev. D **34**, 826 (1986).